

## Sigma Xi, The Scientific Research Society

---

How Microorganisms Move through Water: The hydrodynamics of ciliary and flagellar propulsion reveal how microorganisms overcome the extreme effect of the viscosity of water

Author(s): George T. Yates

Reviewed work(s):

Source: *American Scientist*, Vol. 74, No. 4 (July–August 1986), pp. 358–365

Published by: [Sigma Xi, The Scientific Research Society](#)

Stable URL: <http://www.jstor.org/stable/27854249>

Accessed: 18/07/2012 14:21

---

Your use of the JSTOR archive indicates your acceptance of the Terms & Conditions of Use, available at <http://www.jstor.org/page/info/about/policies/terms.jsp>

JSTOR is a not-for-profit service that helps scholars, researchers, and students discover, use, and build upon a wide range of content in a trusted digital archive. We use information technology and tools to increase productivity and facilitate new forms of scholarship. For more information about JSTOR, please contact support@jstor.org.



*Sigma Xi, The Scientific Research Society* is collaborating with JSTOR to digitize, preserve and extend access to *American Scientist*.

<http://www.jstor.org>

# How Microorganisms Move through Water

*The hydrodynamics of ciliary and flagellar propulsion reveal how microorganisms overcome the extreme effect of the viscosity of water*

The various organisms that propel themselves through an aqueous environment span over 19 orders of magnitude in body mass. At one extreme are blue whales, the largest animals ever to inhabit the earth, and at the other are microscopic bacteria. In terms of absolute speed, the larger organisms swim faster; when speeds relative to body size are compared, however, microorganisms are the true champions. Single-celled organisms, typically between 2 and 1,000  $\mu\text{m}$  long, can sustain swimming speeds up to about 100 body lengths per second. Large pelagic fish like tuna can maintain speeds of only about 10 body lengths per second, while the world record for human swimmers is just over one body length per second.

In all cases, an organism accomplishes self-propulsion by putting its body or appendages through periodic movements. After one cycle of the motion, the organism and its appendages return to their original configuration, but the mean body position is moved forward. The types of appendages used, the types of motion employed, and the very nature of the fluid forces encountered differ greatly for the various swimmers throughout the vast size range. This article will concentrate on the movements

of and the forces experienced by the smallest organisms.

A single drop of water from a pond or stream will usually contain hundreds of organisms invisible to the naked eye, a large percentage of which are capable of swimming under their own power. There are more than 50,000 known species of Protozoa alone, with new ones being described at an average rate of more than one a day, and most swim at some stage of their life cycle (Jahn et al. 1979). Besides being found swimming freely, microorganisms commonly occur inside larger organisms, where they exist in symbiotic or parasitic relationships, and some are responsible for disease.

Detailed observations of the movements of these tiny organisms became possible only after the invention of the light microscope. The electron microscope has added a new dimension to the study of their motility, by providing sharp, highly magnified fixed images for close examination of the microstructures associated with locomotion. With the aid of these powerful tools, cilia and flagella have been identified as the cellular appendages whose movements are most frequently responsible for self-propulsion of microorganisms (Fig. 1).

To appreciate fully how propulsion is achieved by ciliary and flagellar activity, it is essential to understand some fundamental principles of hydrodynamics. After a brief review of the relevant principles, we will look at the structures of cilia and flagella. With knowledge of both fluid dynamics and biology in hand, we will then be able to discuss the mechanics of propulsion in detail. This subject, a subdivision of biofluidynamics, is by its very nature interdisciplinary; it requires collaboration by

the various fields of engineering, physics, applied mathematics, and biology (see for example Gray and Hancock 1955; Holwill 1966; Wu et al. 1975; Brennen and Winet 1977).

## The effects of viscous flows

The larger and more familiar free-swimming animals, such as fish and cetaceans, derive their propulsive thrust by accelerating water backward, taking advantage of the equal and opposite inertial reaction force to overcome the viscous fluid force which would otherwise slowly arrest their motion. The dominance of inertial forces in these cases is evident from the maneuvers of a large ship approaching a harbor. As an experienced mariner will explain, the ship's power must be turned off, or even reversed, well before the ship reaches the dock, because the action of viscosity on the hull only gradually affects the ship's overwhelming momentum.

The ratio of inertial to viscous forces in fluid flows is indicated by a nondimensional quantity called the Reynolds number. For a body of dimension  $L$  moving with velocity  $U$  in a viscous fluid, the inertial force is proportional to  $\rho(UL)^2$ , the viscous force varies like  $\mu UL$ , and the Reynolds number is defined as  $Re = \rho UL / \mu$ , where  $\rho$  is the density and  $\mu$  the viscosity of the surrounding fluid. For fish or humans, the Reynolds number is typically about one million, and inertia dominates the fluid motion. As the body dimension diminishes to the scale of microscopic organisms, viscous forces dominate inertial forces, and the Reynolds number becomes 0.1 or smaller. At the even smaller dimension of the individual cilia and flagella, which

*George T. Yates is Senior Scientist in Engineering Science at Caltech. He received his B.S. from Purdue University and his M.S. and Ph.D. from Caltech. His research focuses on fundamental fluid mechanics, with special emphasis on biofluidynamics. His current interests include the mechanics and physiology of swimming and flying, optimal energy extraction from winds and currents, and free surface flows. The work described in this paper has been carried out with support from the National Science Foundation and the Office of Naval Research. Address: Engineering Science, Caltech, Pasadena, CA 91125.*

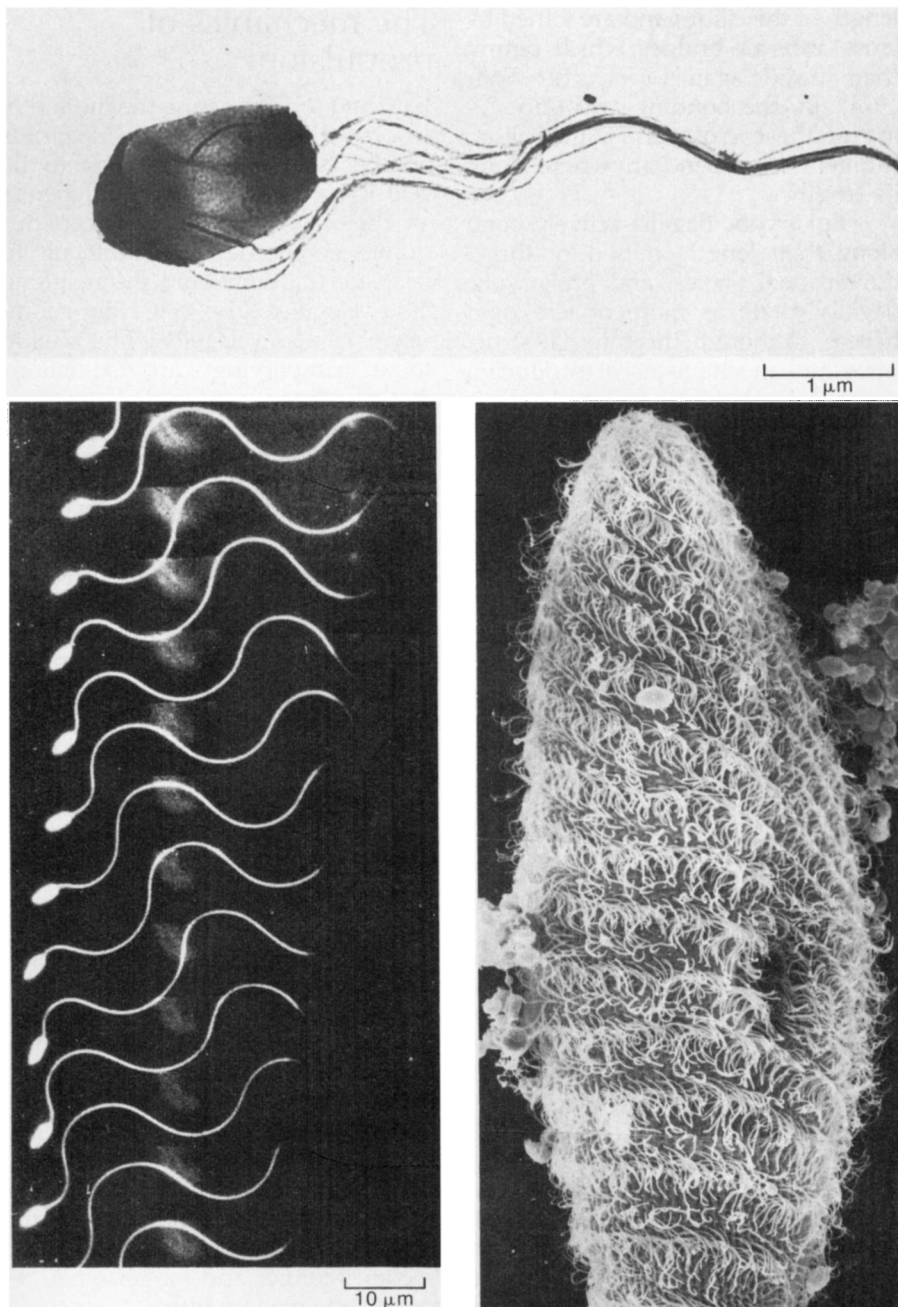


Figure 1. Cilia and flagella are the appendages that propel microorganisms through water. They are distinguished from each other by their length relative to the cell body, as well as by their structures and characteristic movements. Flagella are often attached to one end of the body, and are frequently more than twice the length of the body. The bacterium *Salmonella abortus-equi* (top) has many flagella, which form a bundle that is clearly visible behind the cell body in this electron micrograph. The bundle intermittently unwraps and reforms, thus changing the swimming direction. A spermatozoon from a sea squirt *Ciona* (bottom left) is shown swimming in sea water in this series of flash photographs (top to bottom, 200 flashes per second) taken with a light microscope. The propulsive wave is planar and propagates to the right along the flagellum. Consequently, the cell moves to the left. Cilia (bottom right), which are usually much shorter than the body, are numerous and arranged in rows on the body surface. Gradual variation in the phase of the beat cycle along the length of the cell leads to the coordinated wave pattern seen in this scanning electron micrograph of the microorganism *Paramecium*. (Top photograph from Routledge 1975; bottom left photograph from Omoto and Brokaw 1982; bottom right photograph from Tamm 1972.)

oscillate typically between 10 and 30 cycles per second, the Reynolds number is usually less than  $10^{-5}$ . Because the inertial effects are of no significance at these small scales of motion, microorganisms are unable to take advantage of the inertial reaction and must derive their forward thrust from viscous reactions.

The typical viscous forces which act on a human swimmer are at least 6 orders of magnitude smaller than the inertial forces. To appreciate the nature of the viscous forces experienced by microorganisms, we would have to swim in a fluid one million times more viscous than water. Even in a pool filled with honey the relative strength of viscous to inertial forces would be two orders of magnitude smaller than it is for microorganisms swimming in water, and a more appropriate fluid would be molasses or even tar.

Whenever the Reynolds number is small, the rate of change in momentum over time can be neglected relative to the viscous and pressure components, and time becomes simply a parameter. This means that the fluid motion generated in response to a microorganism's movement depends on its instantaneous velocity, and not on its velocity at any previous instant or on the rate of change of any other quantity with time. Furthermore, because the fluid inertia (mass times acceleration) is negligibly small, any external force must be balanced by the viscous stress and the pressure in the fluid.

We can now begin to appreciate the difficulties encountered in achieving self-propulsion at low Reynolds numbers. For a swimmer—for example, a human in an ocean of molasses—who moves his arms from a given starting position to a final configuration, the instantaneous fluid force depends linearly on the velocity of the body motions. When the swimmer stops moving, not only does his absolute motion stop, but all the surrounding fluid comes to rest immediately, because there are no inertial effects. Furthermore, if the swimmer exactly retraces the paths followed by his arms to their initial configuration, he will find himself (and the fluid) in exactly the same position from which he started. How then can living creatures accomplish self-locomotion under such condi-

tions? The answer to this question lies in the detailed dependence of the viscous forces on the flow velocity and orientation, which I will discuss after looking at the tools nature has provided to enable microorganisms to swim freely in their environment.

## The structures of cilia and flagella

The etymology of the terms cilium and flagellum indicates not only the appearance of these structures but also the type of movement they perform. "Cilium" is derived from the Latin word meaning eyelid, and brings to mind many closely spaced hairs capable of rapid, synchronized movement. "Flagellum" comes from the Latin word for whip, suggesting a long, flexible rope which can be made to move in a wide variety of ways. A closer examination of both the structure and the movement of cilia and flagella reveals some important differences which give them special advantages over eyelashes or whips.

In both prokaryotes (bacteria) and eukaryotes (organisms that have their cell nuclei enclosed in a membrane, such as protozoans and algae) and in the sperm cells of higher animals, the propulsive organelle has traditionally been called a flagellum, but it is now considered a form of cilium in eukaryotes (Jahn et al. 1979). The relatively rigid, helical-shaped flagella of bacteria are about  $0.02 \mu\text{m}$  in diameter and are constructed from subunits of a protein called flagellin with a core about  $0.003 \mu\text{m}$  in diameter. Although it varies greatly from species to species, the length of a bacterial flagellum is almost always more than 100 times its thickness. A rotary joint attaches the flagellum to the cell body and allows it to rotate during locomotion (Berg 1975; Routledge 1975; Macnab and Aizawa 1984).

Cilia, eukaryotic flagella, and the flagella of sperm cells all have essentially the same anatomy, which differs greatly from that of bacterial flagella. Nine outer pairs of microtubules surround a central pair of microtubules, all contained within a roughly circular cross section about  $0.2 \mu\text{m}$  in diameter. These microtubules can bend but are nearly inextensible. They run almost the entire

length of the cilium and are joined by cross arms or bridges which permit them to slide against each other (Satir 1974). By the bonding and unbonding of these cross arms, the cilium can generate a bend anywhere along its length.

Eukaryotic flagella actively bend along their length in two- or three-dimensional waves, and prokaryotic flagella rotate as more or less rigid helices. Although the internal structures and mechanisms of producing motion of eukaryotic and prokaryotic flagella are greatly different, we will consider the mechanics of propulsion of both classes together. The single or multiple flagella of these microorganisms are relatively long (at least one-half and frequently considerably more than the length of the body) and are often attached to one end of the body. The body length of flagellates rarely exceeds  $50 \mu\text{m}$ , while their flagella are often longer than  $100 \mu\text{m}$ .

Cilia are relatively short (much less than the body length), are usually numerous, and are arranged in rows on the body surface. In terms of overall body size, ciliates are generally larger than flagellates, with some species attaining lengths of 1 to 2 mm. The individual cilia have a fairly regular beat pattern with two distinct phases. The forward (power or effective) stroke is rapid, with the cilium fully extended. The return (recovery) stroke, which appears as if a bend were propagated from the base to the tip of the cilium, is slower, with the cilium bent close to the cell surface. As we shall see, this asymmetry in the beat is an essential feature for effective functioning of the cilium.

Because the phase of the beat cycle varies gradually from one cilium to another over the body, an organized wave is observed. This wave may travel in the same direction as the effective stroke or in an opposite direction. The types of both wave and beat patterns are widely varied among the numerous species of ciliates. The control of the coordinated motions of the cilia in these single-celled organisms, which lack a nervous system, remains largely unknown. The most likely underlying mechanisms include changes in membrane potentials or ion concentrations, with or without hydrodynamic coupling.

## The mechanics of propulsion

The fluid force resisting the motion of an object moving at a low Reynolds number is linearly proportional to the velocity of the object, and depends on the flow orientation. Except for simple geometries, it is difficult to calculate this force and the resulting fluid velocities. The long, thin geometry of cilia and flagella lends itself to some simplifying approximations that have been used to develop resistive force theory and slender body theory. These two theories have been highly successful in explaining the mechanics of ciliary and flagellar propulsion.

For objects that are much longer than they are wide and have circular cross sections, the fluid force per unit length is conveniently split into a longitudinal force ( $F_s$ ) and a transverse force ( $F_n$ ). These two components of force can be estimated from the formulas

$$F_s = -\mu C_s U_s$$

and

$$F_n = -\mu C_n U_n$$

where  $U_s$  and  $U_n$  are the tangential and normal velocities of the particular cross section relative to the fluid. The constants of proportionality  $C_s$  and  $C_n$  are generally different and depend on the shape of the body, but are independent of the fluid viscosity  $\mu$  and the velocities  $U_s$  and  $U_n$ . The ratio of the force coefficients  $\gamma = C_s/C_n$  takes on the value 1 for a sphere and approaches 0.5 in the limiting case of a slender body that becomes longer and longer while retaining the same width.

These two formulas constitute the basis of resistive force theory. The essential features of this theory are illustrated in Figure 2, where it is applied to the settling of a long, thin rod inclined at an angle  $\alpha$  from the horizontal. The buoyancy force  $F_b$ , the object's mass times the acceleration of gravity minus the hydrostatic pressure force, acts downward and, in the absence of inertia, must be balanced by the viscous fluid forces. The surprising result is that the rod does not fall straight down in the direction of the buoyancy force but rather has a component of velocity perpendicular to gravity. This lateral migration of the rod occurs only

when  $\gamma < 1$  and becomes more pronounced as  $\gamma$  becomes smaller.

The possibility of self-propulsion is a direct result of  $\gamma$  being less than one. Take the example of an ice skater who is in the middle of a pond and wishes to reach the bank without lifting his skates off the ice. If the skater were to use a pair of poorly designed skates for which  $C_s = C_n$  ( $\gamma = 1$ ), then the resistive force would be aligned parallel to the motion and he would be unable to produce a net forward movement, no matter how hard he tried. Making application of the results shown in Figure 2, he should use a pair of skates that have a very small resistance to movement parallel to the blades (small  $C_s$ ) and that have a very large resistance to sideways movement (large  $C_n$ ). By holding his feet at an outward-pointing angle and pushing them apart, he will begin to move forward (just as the rod in Figure 2 drifts laterally). When he pulls his feet back together, he should point his toes inward to produce a further forward propulsion.

The major strengths of resistive force theory are its simplicity and relative ease of application for obtaining approximate results. Its weaknesses are that appropriate values for the resistive force coefficients are not always obvious, the local fluid velocities are not predicted, and interactions between the flagellum and the cell body or flow boundaries are difficult to account for in a systematic manner. The more rigorous slender body theory overcomes these difficulties and provides a systematic method of approximating the flow field and hence the forces on long, thin objects. Slender body theory is based on the fundamental concepts of mass and momentum conservation at low Reynolds numbers, which result in a system of linear partial differential equations, the so-called Stokes equations. These equations, with appropriate boundary conditions, can be solved in a variety of ways; I will outline only one approach which has been successfully applied to the swimming of microorganisms. The advantage of slender body theory is that solutions of desired accuracy can be obtained, and its disadvantage is that it can require tedious and involved computations.

It should be emphasized that

Stokes equations are linear in the fluid velocity and therefore allow the use of a general solution technique known as the singularity method. This technique is commonly applied to problems throughout engineering and science when the governing equations are linear. If two different solutions of Stokes equations are known, say  $u_1$  and  $u_2$ , then a third solution  $u$  can be found by taking a linear combination of these two ( $u = Au_1 + Bu_2$ , where  $A$  and  $B$  are arbitrary constants). The process can be repeated again and again, and thus a few relatively simple fundamental solutions can be used to construct a whole family of solutions. In the present application, various fundamental solutions can be distributed along the cilia or flagella, cell body, and flow boundaries, and the result-

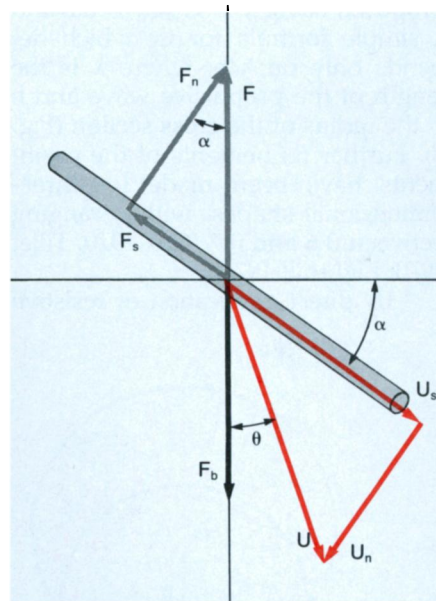


**Figure 2.** Resistive force theory helps explain the fluid forces acting on an organism whose movement is dominated by viscous effects. The theory is illustrated here by an inanimate object, a long, slender rod settling under the action of gravity at a low Reynolds number. The rod migrates laterally as it falls. The net buoyancy force  $F_b$  is balanced by the fluid resistive force  $F$ , which has two components, one normal ( $F_n$ ) and the other tangential to the rod ( $F_s$ ). These forces are linearly proportional to the normal and tangential components of the rod's velocity,  $U_n$  and  $U_s$ , respectively. A simple relation between  $\alpha$  and  $\theta$  results from the quotient  $F_s/F_n$ , and depends only on the ratio of the force coefficients  $\gamma = C_s/C_n$ . By symmetry, whenever  $\alpha$  is  $0^\circ$  or  $90^\circ$ ,  $\theta$  is zero, and thus  $\theta$  must have a maximum for some intermediate values of  $\alpha$ . For  $\gamma = 0.5$ , this occurs when  $\alpha \approx 35^\circ$  and results in a maximum lateral migration of the rod with  $\theta \approx 19^\circ$ .

ing combined flow may represent the swimming of a microorganism.

As a basic building block, we will use a solution of Stokes equations which corresponds to placing a point force with a given magnitude  $F = 8\pi\mu\alpha$  in the fluid. The fundamental singular solution of this problem, called a stokeslet (Figs. 3 and 4), has a velocity field which decays like  $1/r$ , where  $r$  is the distance from the external force to the measuring point. This extremely slow decrease of velocity with distance from the disturbance is especially noteworthy: it indicates that the stokeslet will have a far-reaching influence on the flow field.

If we allow mass to be created at a point inside the flow field, Stokes equations admit another singular solution, a source (Fig. 4), which has a radially outward flow velocity that falls off like  $1/r^2$ . A sink is the opposite of a source, having an inward flow velocity. From appropriate combinations of stokeslets, sources, and sinks, other higher-order singularities which satisfy the governing equations can be obtained (Batchelor 1970; Blake 1971; Chwang and Wu 1976). One of these, the potential doublet, is the limiting case of a source and a sink approaching each other. It results in a velocity field which decays like  $1/r^3$ .

A potential doublet with strength  $\beta = a^3U/2$  satisfies the boundary condition of no normal velocity on a sphere of radius  $a$  translating—that is, moving without rotating—with constant velocity  $U$ . This doublet also satisfies Stokes equations; however, there are tangential fluid velocities on the sphere surface, which are impossible in viscous flows. For an object moving at a low Reynolds number, the fluid velocity at the body surface must be equal to the velocity of the body, a requirement called the no-slip boundary condition. This condition can be satisfied for a sphere by linearly superposing a stokeslet of strength  $\alpha = 3aU/4$  and a doublet of strength  $\beta = -a^3U/4$  (Fig. 3). The importance of the stokeslet strength is seen when we consider the resulting fluid force found by integrating the stresses over the surface of the sphere, which yields the Stokes drag formula

$$F = -8\pi\mu\alpha = -6\pi\mu aU$$

From this we note that the mean stokeslet strength is directly related to the mean external force acting on the body. This association remains valid for all bodies undergoing general motions at a low Reynolds number.

More difficult problems can be solved by distributing the various singularities within a body or on the body surface, and by adding together the velocity fields from all the singularities. The strengths of the singularities are chosen so that the no-slip boundary condition on the body surface is satisfied. Evaluating the strengths involves solving a complicated system of integral equations.

The slenderness of cilia and flagella allows the flow singularities to be distributed along an organelle's center line. It further permits all the singularities except stokeslets outside a certain "near field" region to be neglected, and thus the integral equations are greatly simplified. Velocities due to distant singularities decay rapidly with distance and make only higher-order contributions. The stokeslet must be retained along the entire body length, because its velocity field decays very slowly, falling off, as we have seen, like  $1/r$ . The wide-ranging influence of the stokeslets implies that there will be

strong interactions among adjacent cilia, the cell body, and neighboring cells or boundaries, and this in turn causes some difficulty in obtaining analytic results or in carrying out numerical computations.

In approximating the flow field far from the body, we can combine like singularities into equivalent singularities positioned at the center of the cell. Although the detailed flow velocities very close to the body are lost, the overall fluid flow as seen some distance from the organism can be easily estimated by only one or two equivalent singularities (Fig. 5).

### How flagellates and ciliates swim

Using resistive force coefficients, Hancock (1953) and Gray and Hancock (1955) made major contributions to research on flagellates when they proposed using  $\gamma = C_s/C_n = 0.5$  and a simple formula for  $C_s$  which depends only on  $\lambda/b$ , where  $\lambda$  is the length of the propulsive wave and  $b$  is the radius of the cross section (Fig. 6). Further refinements of the coefficients have been made for three-dimensional shapes, with  $\gamma$  ranging between 0.6 and 0.7 (Cox 1970; Tillet 1970; Lighthill 1976).

By direct application of resistive

force theory to each differential element along the length of a flagellum, Gray and Hancock were able to estimate the fluid force and moment per unit length. The total force and moment are then obtained by summing the contribution from each element. If the organism is self-propelling, the total mean thrust of the flagellum (the total mean fluid force in the direction of motion) must be equal to the drag of the head, which is approximated by the drag on a sphere of radius  $a$ —the Stokes drag formula noted above.

The rate of work done by the flagellum per unit length amounts to  $C_n(U_n)^2 + C_s(U_s)^2$ . When this is integrated over the entire flagellum and averaged over time, and the result is added to the rate of work done in moving the head through the fluid, the total mean power consumption of the organism can be found. We can then estimate the efficiency  $\eta$  of this mode of propulsion as the ratio of the mean rate at which useful work is done to the total mean power consumption. Using this definition, Lighthill (1975) has shown that the maximum efficiency of propulsion for a general planar wave is bounded by

$$\eta \leq (1 - \sqrt{\gamma})^2$$

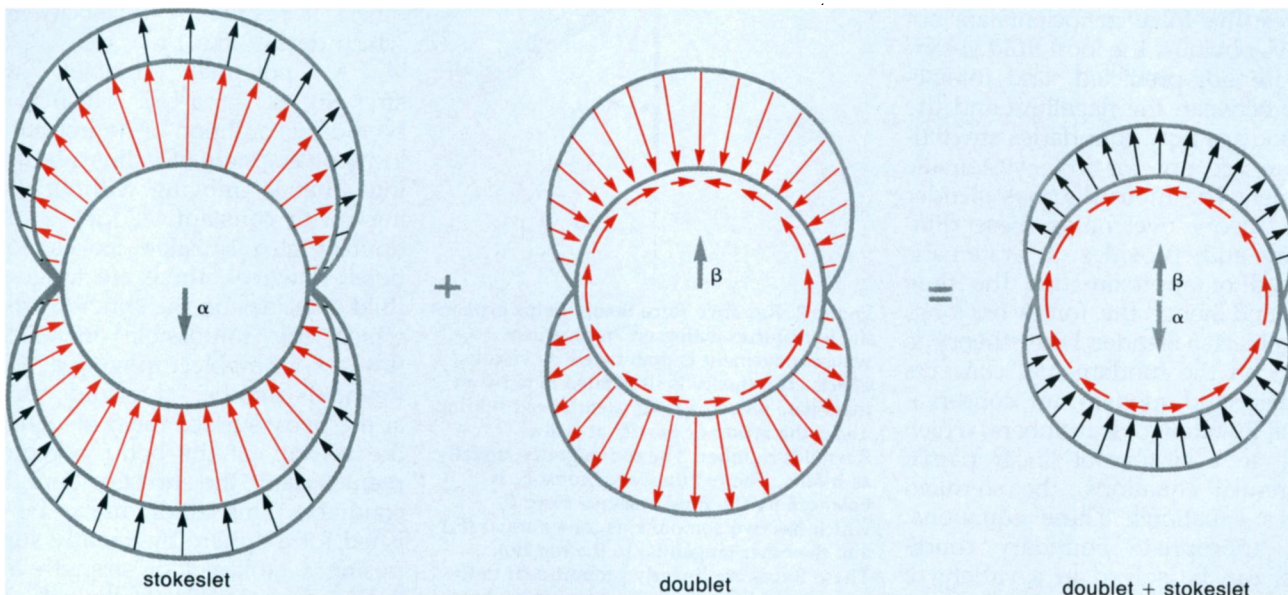


Figure 3. Slender body theory supplements resistive force theory, providing a systematic method of approximating the flow field around an object by solving the Stokes equations with the no-slip boundary condition. The use of flow singularities and the balance of forces in a viscous fluid at low Reynolds numbers are illustrated here by the distribution of fluid forces on an imaginary sphere, which are attributable to the pressure (black arrows) and to viscous forces (color arrows). The viscous forces have two components, a normal stress perpendicular to the surface and a shear stress

tangential to the surface. To conserve linear momentum, the pressure forces, viscous forces, and external forces must always be in equilibrium. For a stokeslet, the viscous forces and the pressure forces combine to balance an external force. In the case of a doublet, the total normal stress exactly balances the net shear stress, and an external force cannot be balanced. The combination of a doublet and a stokeslet of appropriate strengths yields the flow field around the sphere. The stokeslet and doublet have both magnitude and direction (indicated by  $\alpha$  and  $\beta$ ).

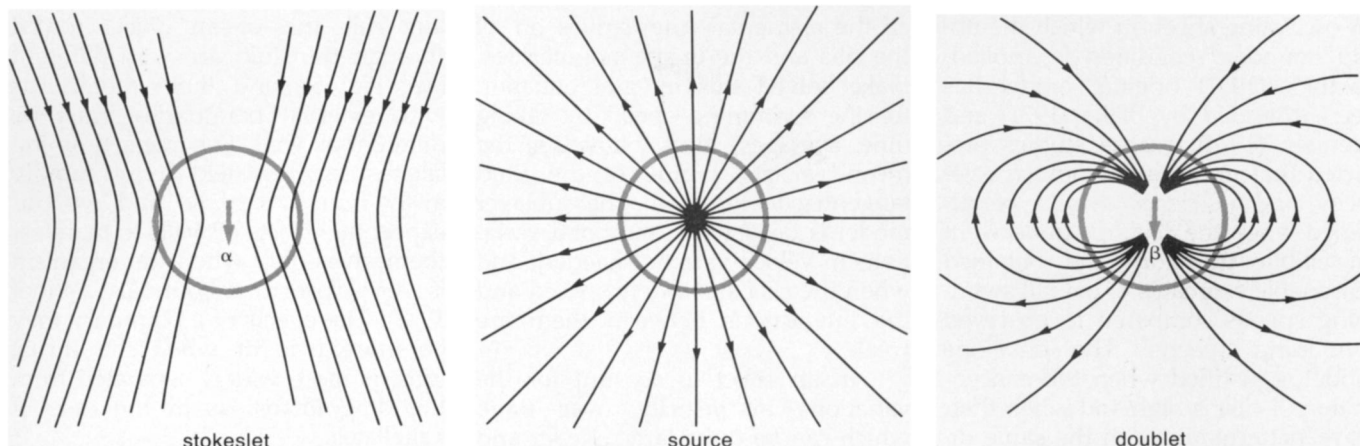


Figure 4. The flow fields resulting from three simple singular solutions of Stokes equations—a stokeslet, source, and potential doublet—are shown here. The magnitude of the fluid velocity varies along the streamlines, decreasing in all cases to zero far from the singularity. The magnitude and direction of the stokeslet and doublet are indicated by  $\alpha$  and  $\beta$ . The circles show the location of the sphere used for evaluating the fluid forces in Figure 3.

Clearly if  $\gamma = 1$ , the propulsive efficiency is zero and no swimming is possible, which agrees with our earlier example of an ice skater. Propulsive efficiency is generally poor for organisms that swim at low Reynolds numbers, because, for  $\gamma = 0.5$ ,  $\eta$  is less than 0.09; it becomes even smaller for larger values of  $\gamma$ .

The force distribution along a planar beating flagellum will vary from thrusting in the regions where the flagellar segments are undergoing transverse motion to drag in the regions where they align nearly parallel with the swimming direction. This variation causes an increased energy consumption for a given thrust (Lighthill 1976). In contrast, a spiral or helical wave generates thrust uniformly along its length and thus may lead to more effective propulsion.

Since they rotate, bacterial flagella must use helical motions for propulsion. Spiral beat patterns are also commonly observed in eukaryotic flagella. For planar beat patterns the linear forces balance; for helical waves, however, the torque must also be balanced, and this requirement cannot be fulfilled without a rotation of the whole organism. Rotation must, in turn, cost the organism additional energy. For organisms with spherical heads and helical flagellar beats, Chwang and Wu (1971) found the optimum head size to range between 10 and 40 times greater than the radius of the flagella. Propulsive efficiencies ranged from 0.10 to 0.28. For organisms with smaller heads ( $a/b$  less than about 5), they concluded that a planar beat

pattern would be more advantageous.

Using slender body theory to study flagellate swimming, Higdon (1979) and Johnson (1980) have found uniformly valid solutions for the entire flow field around microorganisms. Direct comparisons between the resistive force model and slender body theory indicate that if the resistive force coefficients are increased by about 35%, with  $\gamma$  remaining nearly unchanged, better agreement with the more precise slender body theory is obtained (Johnson

and Brokaw 1979).

Three basic models for the propulsion of ciliates have been developed to adapt resistive force and slender body theory to the special characteristics of cilia, their relatively large number, short length, beat pattern, and coordinated movements: the envelope model, the sublayer model, and the traction layer model.

The envelope model assumes that the effects of all the individual cilia can be combined and the instantaneous positions of the cilia tips can be considered as a "body surface,"

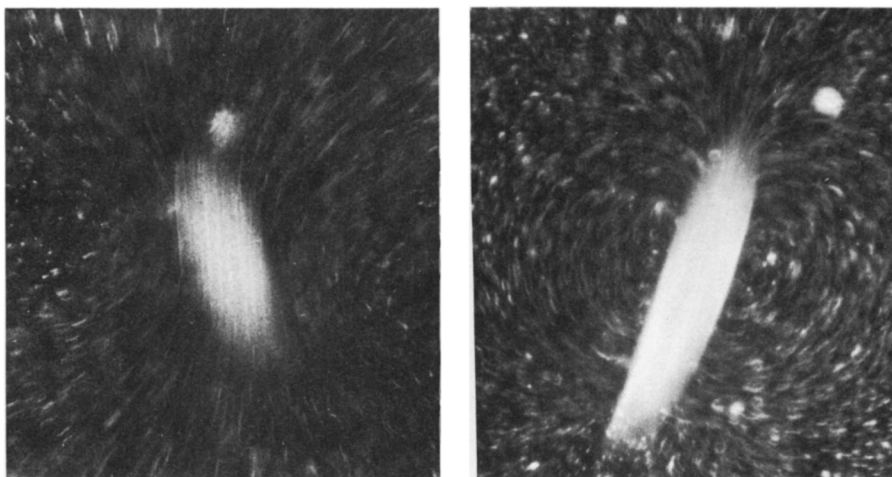


Figure 5. The role of the singular solutions of Stokes equations is illustrated by the marked differences in the flow fields of a free-swimming organism (right) and one being drawn through the fluid by an external force (left). The flow is revealed in these time-exposure photographs by suspended particles 1  $\mu\text{m}$  in diameter. The streaks made by the particles form streamline patterns which can be compared to those in Figure 4. In both the flow pattern created by a dead paramecium (*P. multimicronucleatum*) settling under gravity toward the bottom of the picture and the flow pattern around a living paramecium swimming freely in a horizontal plane toward the lower left, the net stokeslet strength is proportional to the external force acting on the body. For a free-swimming organism, where the external forces are relatively insignificant, the sum of all the viscous forces and thus the resultant stokeslet strength become insignificant. Hence, far from the body, the velocity field behaves like a potential doublet.

an oscillating sheet on which the no-slip boundary condition is applied. Taylor's (1951) original model has been extended by Blake (1971) and Brennen (1974), whose studies predicted that maximum propulsive velocity and efficiency would be attained when the cilia tips underwent an elliptic trajectory and obtained reasonable estimates of overall swimming speeds compared to observed swimming speeds. The envelope model is justified when the concentration of cilia is high and when their wave patterns move in the same direction as the effective stroke. It must be abandoned whenever the flow inside the ciliary layer is to be considered or the assumption of an impermeable surface is violated, as may be the case for wave patterns moving in a direction opposite to the effective stroke and for widely separated cilia.

The sublayer model, first proposed by Blake (1972), addresses the flow within the ciliary layer, where the force on each cilium, and hence the stokeslet strength, is found using slender body theory. Since the cilia operate close to a wall (i.e., the cell body), the singularity types and strengths must be modified. For a single stokeslet above a wall, a system of image singularities, which includes another stokeslet of equal strength but opposite sign and two other higher-order singularities, is needed below the wall to satisfy the no-slip boundary condition on the wall (Blake 1971). The flow field is then represented as an integral over

all the elemental singularities on all the cilia and the image singularities. Blake solved this integral equation for the swimming speed by taking time averages, thus obtaining the mean velocity profile of the fluid tangential to the wall. The sublayer model is used when temporal variations in velocity are not needed, and when the cilia are widely spaced and the interactions between them are weak.

In an effort to account for the variations in velocity over time, which can be quite large, Keller and his colleagues (1975) introduced the traction layer model, which smooths out the ciliary forces to form a continuous body force inside the ciliary layer and retains the oscillatory velocities. The resulting iterative solution shows that the oscillations in velocity are of the same order of magnitude as the mean flow components within the ciliary layer and decay exponentially outside the layer.

## The effects of walls

In nature, motile cells are found both at some distance from and in the immediate neighborhood of walls. Almost all observations of swimming microorganisms are made in the vicinity of solid boundaries in the form of glass microscope slides. Both in nature and in the laboratory, the presence of walls may considerably modify an organism's motions.

The flow fields of a self-propel-

ling cell and of an object forced through the fluid are very different (see Fig. 5), and their interactions with external boundaries must be different as well. For free-swimming ciliates, the flow field decays rapidly away from the body, and we can expect the effects of walls to manifest themselves only when the organism is very close to a boundary (Winet 1973). The effects of a boundary may be more evident when the thrust force is more widely separated from the drag forces, as in the case of flagellates.

The head of a flagellate can be considered as an inert object moving under an external force, and there is no question that, for the same applied force, the velocity will decrease when the head moves close to a solid boundary. At low Reynolds numbers this boundary effect is very strong, and the speed can easily be reduced by more than 5% even when the object is ten head radii from the wall (Lee and Leal 1980).

For a slender body moving near a wall, both the normal and tangential resistive force coefficients increase. It is important to note that  $C_n$  increases proportionally more than  $C_s$ , so that  $\gamma = C_s/C_n$  decreases and may even fall below 0.5 (Yang and Leal 1983). Recalling that propulsion becomes more efficient as  $\gamma$  is reduced, we see that there are two competing effects as a flagellate approaches a solid boundary: one to enhance the performance (increase  $\eta$ ) and the other to retard the motion (increase the drag). The current data are insufficient to tell which effect predominates.

Although data on the swimming speed of flagellates in relation to the distance from a wall are obscured by variations in the speed of individuals and possible changes in the rate of work, several other observations clearly show the important influence of the walls. Flagellates swim in curved paths near a solid boundary. For eukaryotic flagellates the typically three-dimensional beat pattern is flattened and approaches the limiting case of a two-dimensional planar beat. In addition, the beat frequency is noticeably lowered (Katz et al. 1981).

For a flagellate swimming parallel to the wall and using a helical beat pattern, the segments of the flagellum near the wall experience larger

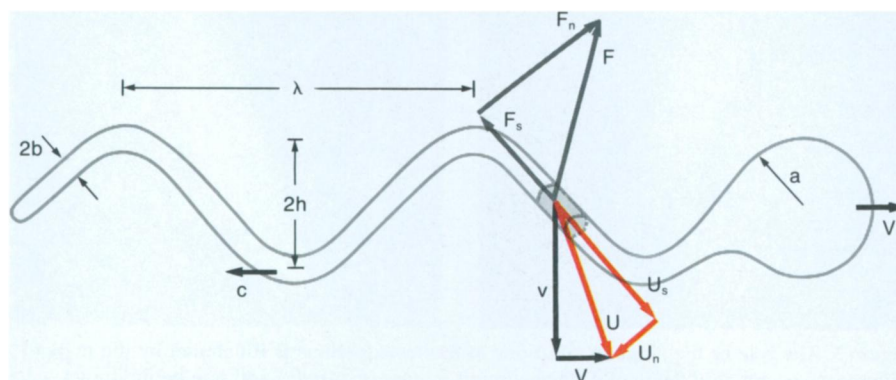


Figure 6. The kinematics of a swimming flagellate are illustrated by an organism with a spherical head of radius  $a$  and a single flagellum of diameter  $2b$ . As the organism moves to the right at a constant mean speed  $V$ , a propulsive wave propagates backward along the flagellum at speed  $c$ . In this simplified example, the flagellum remains in the plane of the page, and both the wave amplitude  $h$  and the wave length  $\lambda$  are constant. The highlighted segment of the flagellum is moving downward with velocity  $v$  in addition to moving forward with velocity  $V$ . The segment's total velocity  $U$  can be resolved into normal and tangential components. The viscous force  $F$  per unit length can be estimated by resistive force theory or by slender body theory. It has a component in the direction of motion (thrust) which, for a free-swimming organism, is balanced by the drag on the head.

forces than those parts away from the wall, and the forces and moments acting on the head are in turn changed. Besides altering the forward speed and the rate of rotation around the direction of swimming, this asymmetrical distribution of forces creates a torque which rotates the organism in the plane of the wall. Thus, free-swimming cells move in curved paths near a wall.

A rigorous analysis of the effects of walls can be accomplished by solving the Stokes equations using distributions of singularities. Blake (1971) constructed an image system for an isolated stokeslet in the vicinity of a rigid wall, and others have expanded on this concept (Yang and Leal 1983). Comparisons between observations and these theories should lead to some interesting work in the future.

Both resistive force theory and slender body theory shed considerable light on the basic features of fluid flows at very low Reynolds numbers. The far-reaching influence of the stokeslet is especially noteworthy, as is its association with the total external force on a body. Microorganisms accomplish self-propulsion as a direct result of the fluid force's dependence on the flow orientation and the asymmetric movement of the organisms' cilia or flagella along periodic paths. Our knowledge remains incomplete, especially regarding the effects of boundaries, interactions among cilia, three-dimensionality of the flows, and swimming in nonlinear fluids such as mucus. There is no doubt that our understanding will continue to be expanded by collaboration among the various branches of biology and engineering and by close interaction between observation and analysis.

## References

- Batchelor, G. K. 1970. Slender body theory for particles of arbitrary cross section in Stokes flow. *J. Fluid Mech.* 44:419-40.
- Berg, H. C. 1975. Bacterial movement. In *Swimming and Flying in Nature*, ed. T. Y. Wu, C. J. Brokaw, and C. Brennen, vol. 1, pp. 1-11. Plenum.
- Blake, J. R. 1971. A note on the image system for a stokeslet in a no-slip boundary. *Proc. Cambridge Phil. Soc.* 70:303-10.
- . 1972. A model for the micro-structure in ciliated organisms. *J. Fluid Mech.* 55:1-23.
- Brennen, C. 1974. An oscillating-boundary-layer theory for ciliary propulsion. *J. Fluid Mech.* 65:799-824.
- Brennen, C., and H. Winet. 1977. Fluid mechanics of propulsion by cilia and flagella. *Ann. Rev. Fluid Mech.* 9:339-98.
- Chwang, A. T., and T. Y. Wu. 1971. A note on the helical movement of microorganisms. *Proc. Royal Soc. London B*178:327-46.
- . 1976. Hydromechanics of low-Reynolds-number flow. Part 4: Translation of spheroids. *J. Fluid Mech.* 75:677-89.
- Cox, R. G. 1970. The motion of long slender bodies in a viscous fluid. Part 1: General theory. *J. Fluid Mech.* 44:791-810.
- Gray, J., and G. J. Hancock. 1955. The propulsion of sea-urchin spermatozoa. *J. Exp. Biol.* 32:802-14.
- Hancock, G. J. 1953. The self-propulsion of microscopic organisms through liquids. *Proc. Royal Soc. London A*217:96-121.
- Higdon, J. J. L. 1979. The hydrodynamics of flagellar propulsion: Helical waves. *J. Fluid Mech.* 94:331-51.
- Holwill, M. E. J. 1966. Physical aspects of flagellar movement. *Physiol. Rev.* 46:696-785.
- Jahn, T. L., E. C. Bovee, and F. F. Jahn. 1979. *How to Know the Protozoa*. 2nd ed. Wm. C. Brown.
- Johnson, R. E. 1980. An improved slender-body theory for Stokes flow. *J. Fluid Mech.* 99:411-31.
- Johnson, R. E., and C. J. Brokaw. 1979. Flagellar hydrodynamics. A comparison between resistive-force theory and slender-body theory. *Biophys. J.* 25:113-27.
- Katz, D. F., T. D. Bloom, and R. H. BonDurant. 1981. Movement of bull spermatozoa in cervical mucus. *Bio. Reproduction* 25:931-37.
- Keller, S. R., T. Y. Wu, and C. Brennen. 1975. A traction layer model for ciliary propulsion. In *Swimming and Flying in Nature*, ed. T. Y. Wu, C. J. Brokaw, and C. Brennen, vol. 1, pp. 253-72. Plenum.
- Lee, S. H., and L. G. Leal. 1980. Motion of a sphere in the presence of a plane interface. Part 2: An exact solution in bipolar coordinates. *J. Fluid Mech.* 98:193-224.
- Lighthill, M. J. 1975. *Mathematical Biofluidynamics*. SIAM.
- . 1976. Flagellar hydrodynamics: The John von Neumann lecture, 1975. *SIAM Rev.* 18:161-230.
- Macnab, R. M., and S.-I. Aizawa. 1984. Bacterial motility and the bacterial flagellar motor. *Ann. Rev. Biophys. Bioeng.* 13:51-83.
- Omoto, C. K., and C. J. Brokaw. 1982. Structure and behaviour of the sperm terminal filament. *J. Cell Sci.* 58:385-409.
- Routledge, L. M. 1975. Bacterial flagella: Structure and function. In *Comparative Physiology—Functional Aspects of Structural Materials*, ed. L. Bolis, H. P. Maddrell, and K. Schmidt-Nielsen, pp. 61-73. North-Holland.
- Satir, P. 1974. The present status of the sliding micro-tubule model of ciliary motion. In *Cilia and Flagella*, ed. M. A. Sleight, pp. 131-42. Academic.
- Tamm, S. L. 1972. Ciliary motion in *Paramecium*. *J. Cell Bio.* 55:250-55.
- Taylor, G. I. 1951. Analysis of the swimming of microscopic organisms. *Proc. Royal Soc. London A*209:447-61.
- Tillett, J. P. K. 1970. Axial and transverse Stokes flow past slender axisymmetric bodies. *J. Fluid Mech.* 44:407-17.
- Winet, H. 1973. Wall drag on free-moving ciliated micro-organisms. *J. Exp. Biol.* 59:753-66.
- Wu, T. Y., C. J. Brokaw, and C. Brennen, eds. 1975. *Swimming and Flying in Nature*, vols. 1 and 2. Plenum.
- Yang, S. M., and L. G. Leal. 1983. Particle motion in Stokes flow near a plane fluid-fluid interface. Part 1: Slender body in a quiescent fluid. *J. Fluid Mech.* 136:393-421.

